

Deepti Hariharan, Kanikode Abdul Latheef Abdul Rahman
Group P3

Advanced Lab Course: Photometry of Star Clusters – S263

30 August 2019
Tutors: Dang Thanh Nhan Nguyen & Sangwoo Park
Universität Bonn

Contents

1	Introduction	5
1.1	Star Clusters	5
1.2	HRD/CMD	6
1.3	Observables	6
1.3.1	Apparent Magnitude	6
1.3.2	Distance Modulus	7
1.4	Instrumentation	7
1.4.1	Telescope Optics	7
1.4.2	CCD Detector	8
2	Observations	9
2.1	Science Frames	9
2.2	BIAS Frames	9
2.3	DARK Frames	9
2.4	FLAT Frames	10
3	Data Reduction	13
3.1	THELI	13
3.2	SExtractor	13
4	Analysis	15
4.1	Open Cluster	15
4.1.1	Calibration	15
4.1.2	Distance Determination	16
4.1.3	Isochrone Fitting	16
4.2	Globular Cluster	18
4.2.1	Distance Determination	19
4.2.2	Isochrone Fitting	20
5	Conclusion	23

1 Introduction

Star clusters are groups of gravitationally bound stars. They give information about evolution of a population of stars at a particular phase (age, distance and metallicity) in their lifetime. This can be done with the help of theoretical models like the Hertzsprung-Russell Diagram (HRD). The HR diagram plots the magnitude of stars against their spectral class. The Color-Magnitude Diagram (CMD) is a derivative of the HRD which plots the apparent magnitudes against color.

1.1 Star Clusters

Star clusters are formed from giant molecular clouds which collapse to form clumps and later develop into stars. The clumps largely consists of hydrogen and helium and a smaller quantity of heavier elements. 10–30% of the gas in the cloud is used for star formation. The masses of stars, m follow the Initial-Mass Function (IMF) canonically given by:

$$\begin{aligned}\xi(m) &= 0.237 m^{-1.35} \text{ for } m \leq 0.5M_{\odot} \\ \xi(m) &= 0.114 m^{-2.35} \text{ for } m > 0.5M_{\odot}\end{aligned}\tag{1.1}$$

Observation of pre-main-sequence stars show a primordial binary fraction of 100% which means almost every clump split into two to yield two stars forming a binary system. For a cluster with N_s single stars and N_{bin} binary systems, the binary fraction f_{bin} is defined as:

$$f_{bin} = \frac{N_{bin}}{N_s + N_{bin}}\tag{1.2}$$

Star clusters are classified into two types — open clusters and globular clusters.

Open clusters contain fewer stars and have a diameter of 1–10 pc. They are generally young with ages varying from a few million to 10 billion years. These clusters are more diffuse and lie within the galactic plane. This is because in most spiral galaxies including the Milky Way, only the galactic disc has the conditions necessary to accumulate enough gas to induce gravitational collapse to form stars. Hence, open clusters form continuously in the galactic disc and continue to move around the galactic center in the plane of the host galaxy.

Globular clusters are much larger with diameter 20–150 pc containing 10^4 – 10^7 stars . The are more symmetric and circular than the former and are centrally concentrated. They are older than open clusters and are some of the oldest objects in the universe with ages 11–13 billion years. Unlike open clusters, these are randomly distributed in the galaxy and do not have specified orbits. Globular clusters can only form in rich molecular clouds with high star forming rates (SFR) such as during the Big Bang or galaxy-merging events. Most globular clusters were formed before large structures such as galaxies came into existence and so they are not confined to the galactic plane.

1.2 HRD/CMD

The HR diagram is an important tool used to study stellar evolution. It shows the relation between the absolute magnitude of stars and their spectral class. These quantities are hard to determine, so they were later replaced by temperature-luminosity (theoretical HR diagram) and color-magnitude (observational HR diagram). A typical Hertzsprung-Russell/temperature-luminosity (HRD) or color-

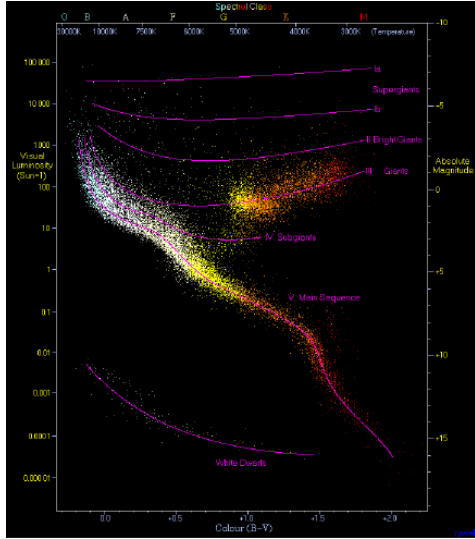


Figure 1.1: HRD/CMD (source: <http://www.atlasoftheuniverse.com/hr.html> cited in [1])

magnitude diagram (CMD) diagram is shown in fig. 1.1.

Most of a star's lifetime is spent in the main-sequence branch. At this stage, the stars burn mostly hydrogen in their cores. When stars run out of hydrogen, they deviate from the main-sequence at the turn-off point into the red-giant branch. The cores of the stars now primarily contain helium and hydrogen will continue to burn around the core. These stars are cooler and are called red-giants. For stars with mass greater than $0.5M_{\odot}$, the core eventually reaches the temperature to start burning helium and the stars move into the horizontal branch.

1.3 Observables

1.3.1 Apparent Magnitude

The apparent magnitude, m , is the measure of the brightness of the star as seen from Earth. It is the integrated radiation flux f in a particular frequency range $\Delta\nu$:

$$m = \int_{\nu_1}^{\nu_2} f d\nu \quad (1.3)$$

The apparent magnitude is a comparative scale of magnitude of the brightness of the star such that:

$$m_1 - m_2 = -2.5 \log_{10} \left(\frac{f_1}{f_2} \right) \quad (1.4)$$

A lot of the intensity of light coming from the star is lost on its way to a telescope located on Earth due to the intergalactic dust, Earth's atmosphere and the limitations of the telescope. Therefore the

flux received by the telescope is given by:

$$f \equiv \int_0^{\infty} f_{\nu} T_{\nu} F_{\nu} R_{\nu} d\nu \quad (1.5)$$

where f_{ν} is the flux that reaches the solar system, T_{ν} is the transmission of the atmosphere, F_{ν} is the transmission of any applied filter and R_{ν} is the efficiency of the telescope system.

The best conditions for observing clusters is achieved at the zenith and at higher altitudes where the light has to travel minimum distance to reach the telescope. These effects are described in terms of the object airmass $a = 1/\cos z$ where z is the angular distance from the zenith.

1.3.2 Distance Modulus

The observed flux decreases as a function of the square of the distance d . Assuming that an object located at distance D has a flux F and apparent magnitude M , the flux f of an object at distance d can be calculated as:

$$f = \left(\frac{D}{d}\right)^2 F \quad (1.6)$$

D is usually assumed to be 10 pc. Using eq. (1.4), the distance modulus $m - M$ can be calculated as:

$$m - M = -2.5 \log_{10}\left(\frac{f}{F}\right) = 5 \log_{10}\left(\frac{d}{D}\right) = 5 \log_{10}d - 5 + A \quad (1.7)$$

where A is the magnitude of interstellar extinction which causes the star to appear dimmer due to absorption and scattering of photons in the interstellar medium. This effect is strongly wavelength dependent and can be determined by taking pictures with different color filters. The distance can then be calculated as:

$$d = 10^{0.2(m-M+5-A)} \quad (1.8)$$

1.4 Instrumentation

1.4.1 Telescope Optics

A 50m Cassegrain reflector telescope as shown in fig. 1.2 placed at the top of Argelander-Institute für Astronomie, Bonn was used for this experiment. It has a f-number of f/9 at its Cassegrain focus and f/3 at its primary focus.

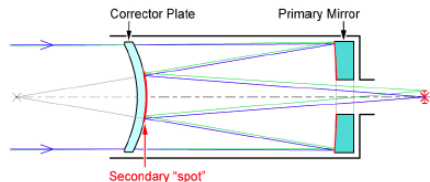


Figure 1.2: A Cassegrain reflector telescope—the CCD camera is placed at the star [1]

Due to diffraction, the image from a point source appears as airy discs. For a circular aperture of diameter D and wavelength of incoming light λ , the angular resolution is:

$$\Delta\theta = 1.22 \frac{\lambda}{D} \quad (1.9)$$

Due to atmospheric effects, the resolution is reduced and can be described by a Gaussian whose FWHM (full width at half maximum) gives the size of the stellar image called 'seeing'. Seeing is best at high altitudes. In Alfa, Bonn, a 2" seeing is achieved.

1.4.2 CCD Detector

Charged Coupled Devices (CCDs) consist of a two-dimensional array of pixels, produced as a light-sensitive metal oxide semiconductor (MOS) capacitor on a silicon substrate. The photons detected are converted to electrons by photoelectric effect. These photo-electrons are then stored in capacitors which are then read-out column-wise to a read-out column by an alternating voltage applied to the pixels. The read-out column is then read out pixel-wise and the signal is amplified and converted to a digital signal.

CCDs are highly advantageous as they have high sensitivity and spectral range. They also have a high linear dynamical range. The digital signal from CCD is also relatively easy to analyze. Some limitations arise due to the dark current, a consequence of temperature fluctuations which causes the CCD pixels to reach their saturation in a short time. Therefore, several short exposures are made to avoid saturation of the pixels. For each exposure, the telescope is moved a few arcseconds. This method is called dithering. Another limitation of CCD are dead pixels which are assigned zero weight in the weighting process.

The CCD used for this experiment is of type SBIG STL-6303E with 3072×2048 pixels and pixel size $9\mu\text{m} \times 9\mu\text{m}$. Each pixel can store 100,000 electrons and has an analog-to-digital (ADU) gain of 1.4 electrons/ADU. It can be thermo-electrically cooled to 30° below room temperature to minimize the dark current. The UBV (ultraviolet, blue and visual) filter system developed by Johnson & Morgan in 1953 was used.

2 Observations

2.1 Science Frames

The images of the objects of interest are called science frames. The science frames were taken using blue, green (visual) and red filters. A science frame of galaxy M92 taken during the night observation is shown in fig. 2.1.

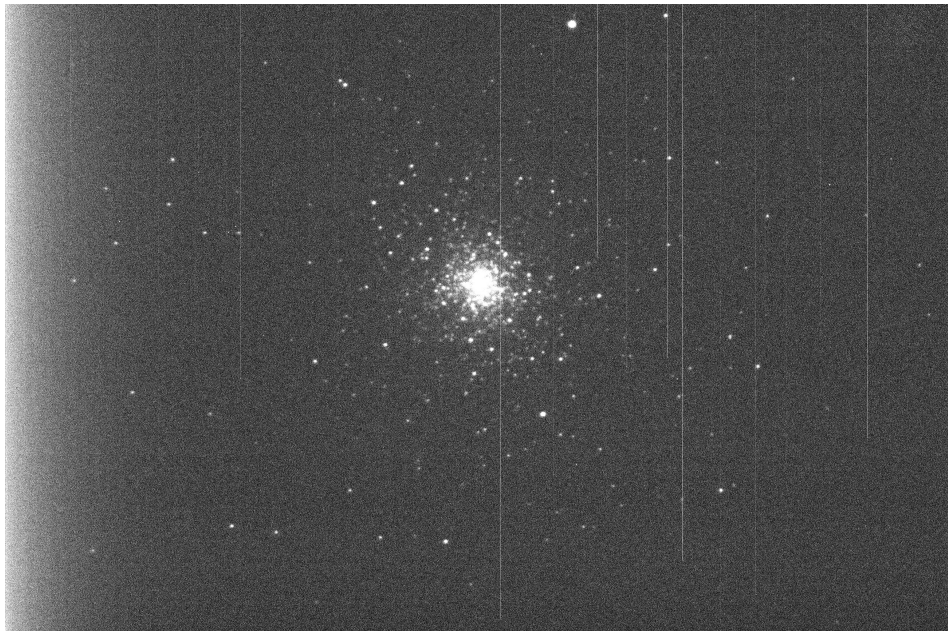


Figure 2.1: Science frame of M92

2.2 BIAS Frames

Pixels with small count has to be very accurate and pixels with large counts does not have to be that accurate for better coverage of the available range of counts. For this purpose, logarithm of the analog signal from the CCD is taken. As the analog-digital converter fails for zero and negative values, an offset is added to the analog signal before logarithm is taken. The BIAS frames are taken at zero-exposure time and subtracted from the science and FLAT frames. BIAS frames indicate the dead pixels as shown in fig. 2.2.

2.3 DARK Frames

Dark current flows through the CCD at all times due to thermal fluctuations even if it is not exposed to optical radiation leading to a fixed-pattern noise. DARK frames are taken without any optical radiation

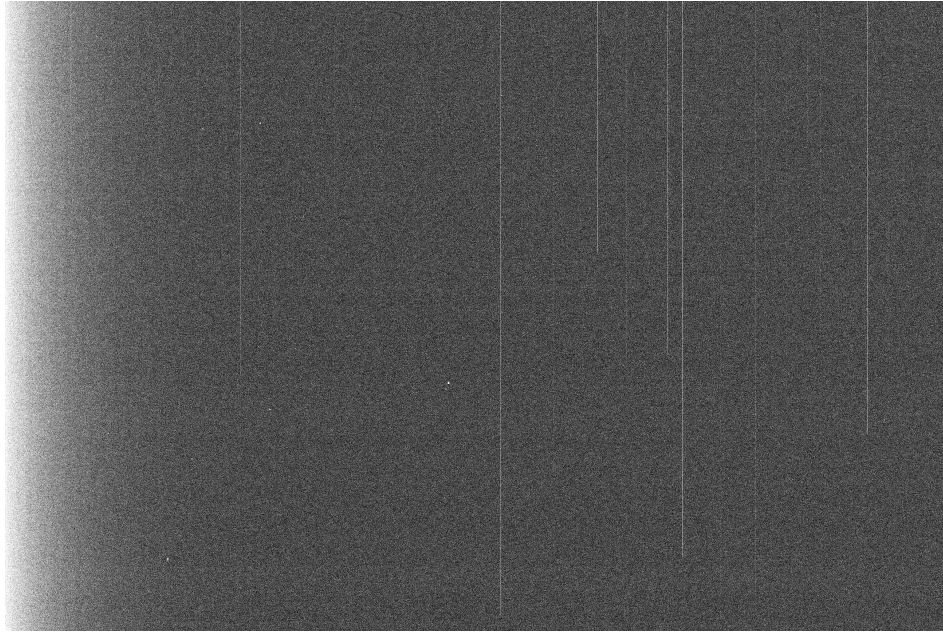


Figure 2.2: A BIAS frame. The white lines indicate the dead pixels; if one pixel goes bad, the entire column deteriorates.

on the cooled CCD with the same exposure time as that of the science frames. They are then subtracted from the science and FLAT frames. A DARK frame taken during the observation is shown in fig. 2.3.

2.4 FLAT Frames

FLAT frames are taken by exposures to a uniformly illuminated background. Because of dust and other variations due to the telescope optics, the frames are not uniform and donut-like shapes are seen as in fig. 2.4. The pixel-wise variation of response is also recorded in the FLAT frame. The exposure level of a FLAT frame is chosen such that the peak brightness is 1/2 or 2/3 of the saturation level. For each filter used to make a science frame, a FLAT frame is made as the pixel response is dependent on the wavelength of the incoming light. The FLAT frames are then normalized to an average value of 1 and used to divide the science frames. Weights are assigned to each pixel such that the bad pixels carry less weight and the good pixels carry more weight. The bad pixels can then be masked with the help of softwares.

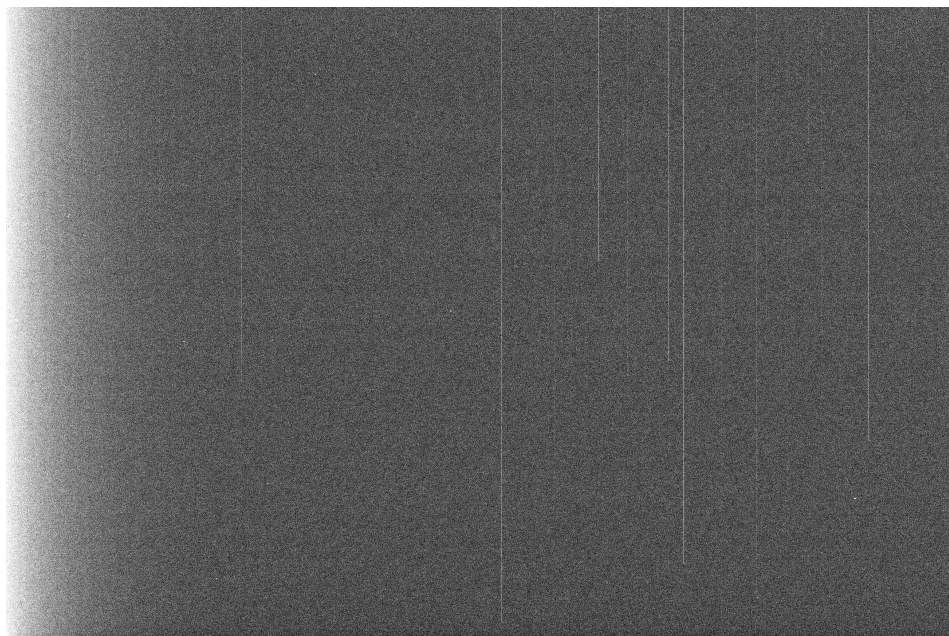


Figure 2.3: DARK frame

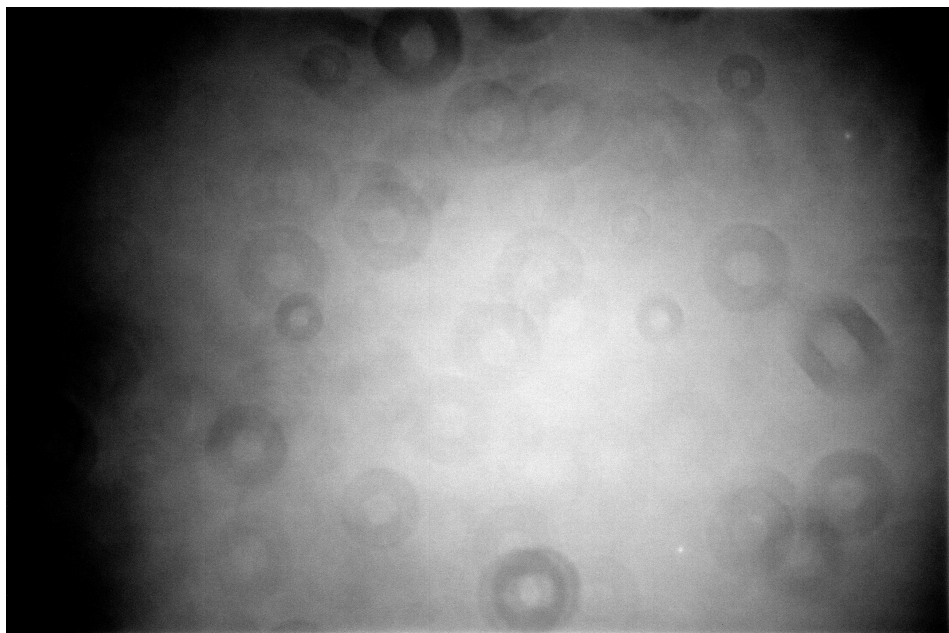


Figure 2.4: FLAT frame

3 Data Reduction

We worked on the data provided by the tutor of the cluster M34 as the data from our observation was not good. The data reduction was done using the GUI version of **THELI**, a freely-available software package for the reduction of astronomical imaging data which was in part developed at AIfA. The magnitudes were then extracted using SExtractor.

3.1 THELI

THELI takes in all the data and processes it to finally give a co-added color image of the cluster. First, the BIAS and DARK frames were split to create a master BIAS and master DARK frame. The FLAT frames were then processed, i.e., overscan corrected, BIAS subtracted and scaled. The science frames were then using the processed BIAS, DARK and FLAT frames. Weighting was done to assign appropriate weight to the pixels. Then, astrometric calibration was done to connect the pixel coordinates with the sky coordinates using a catalog. The remaining sky background was subtracted to create a clear picture and the images co-added. This process was done for all the filters to finally give a RGB color image as shown in fig. 3.1.

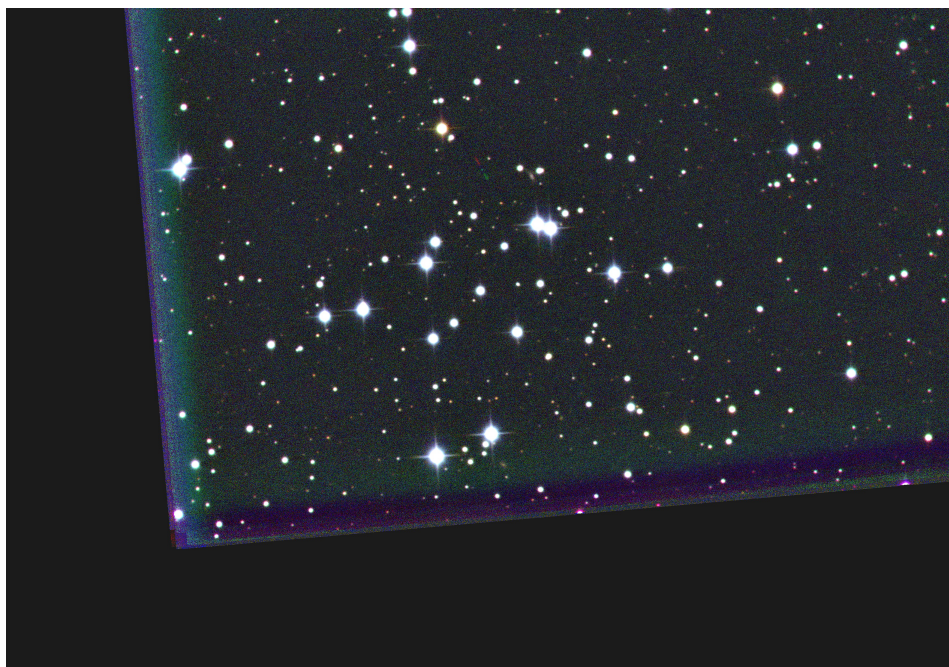


Figure 3.1: RGB image of cluster M34

3.2 SExtractor

SExtractor extracts the source catalog of the objects from the image. The catalogs of the three filters are created and cross referenced and only the sources detected in all three filters are extracted.

4 Analysis

Analysis was done for the open cluster M34 and three globular clusters GC1, GC2 and GC3. The age, distance and metallicity was determined for each cluster by isochrone fitting using Python. Isochrones are theoretically drawn assuming the stars are at a distance of 10pc and so they have a narrow width. Therefore, the fit results are only approximate and not exact.

4.1 Open Cluster

The CMD was plotted for the cluster with the visual apparent magnitude (M_V) in the y-axis and the difference between blue and visual magnitudes (B-V) in the x-axis as shown in fig. 4.1.

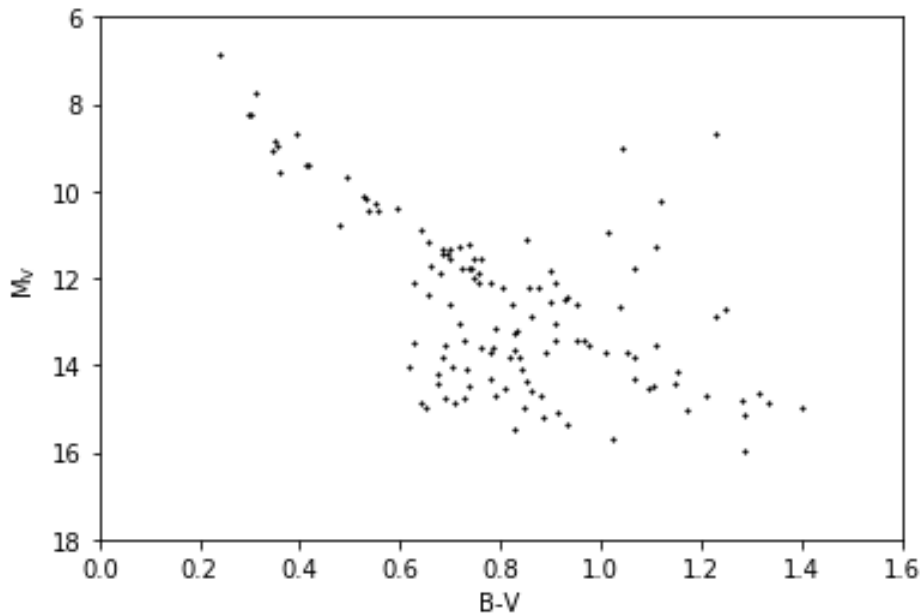


Figure 4.1: CMD of open cluster

4.1.1 Calibration

The magnitudes in the catalog obtained from data reduction was not calibrated. The measured magnitude of the stars were compared with reference magnitudes from an astronomical database [2]. This was done by hand for about 30 stars and averaged. A constant shift of 0.487 was added to the B-magnitude and 1.077 to the V-magnitude and the CMD was plotted (fig. 4.2).

The extinction factor A was assumed to be zero as it is much smaller then the accuracy of magnitude achieved in Bonn due to light pollution and telescope configuration.

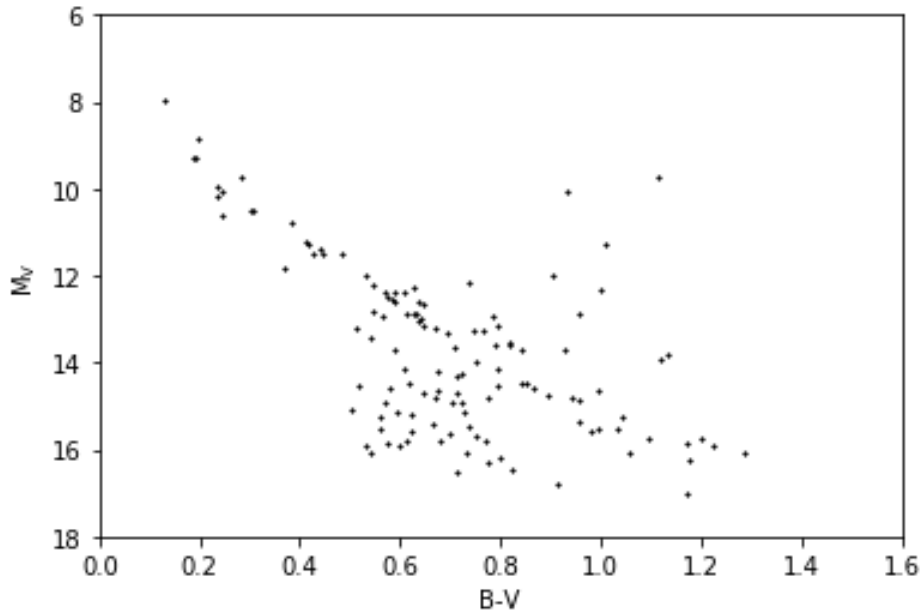


Figure 4.2: Calibrated CMD of open cluster

4.1.2 Distance Determination

Open clusters of young age have a well-defined main-sequence which does not vary significantly with metallicity. An isochrone was fitted to the calibrated CMD after applying a shift to the V-magnitude of the isochrone such that the high-mass part of the main sequence fits the CMD. The shift needed was 8.1 ± 0.25 . This shift corresponds to the distance modulus $m - M$. The distance d was then calculated using eq. (1.8) and the error:

$$\Delta d = 0.2 \ln 10 \times \Delta(m - M) \times d \quad (4.1)$$

The distance was found to be (416.87 ± 11.52) pc.

4.1.3 Isochrone Fitting

The calibrated CMD was fit with isochrones provided from the Geneva database to see which parameters reproduce the isochrone best.

Age

To find the age of the cluster, the CMD was fitted with the isochrones of constant metallicity and different ages as shown in fig. 4.3. The age is indicated by the turn-off point. The age was found to be (245.7 ± 51.55) Myr. The error was calculated by looking at the difference between the previous and next isochrone as the proper fit probably lies between those two.

Metallicity

The metallicity of the cluster can be determined by looking at the main sequence of stars. Isochrones of different metallicities and constant age was fit to the CMD as shown in fig. 4.4. The best fit was achieved for $Z = 0.1$. There is no error in this value as the given theoretical metallicites were fixed.

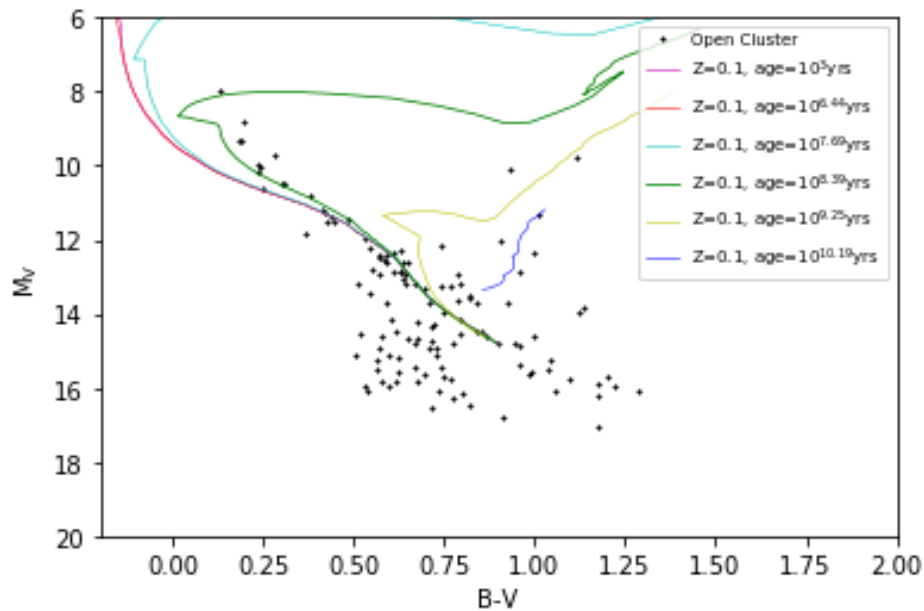


Figure 4.3: Determination of age of open cluster

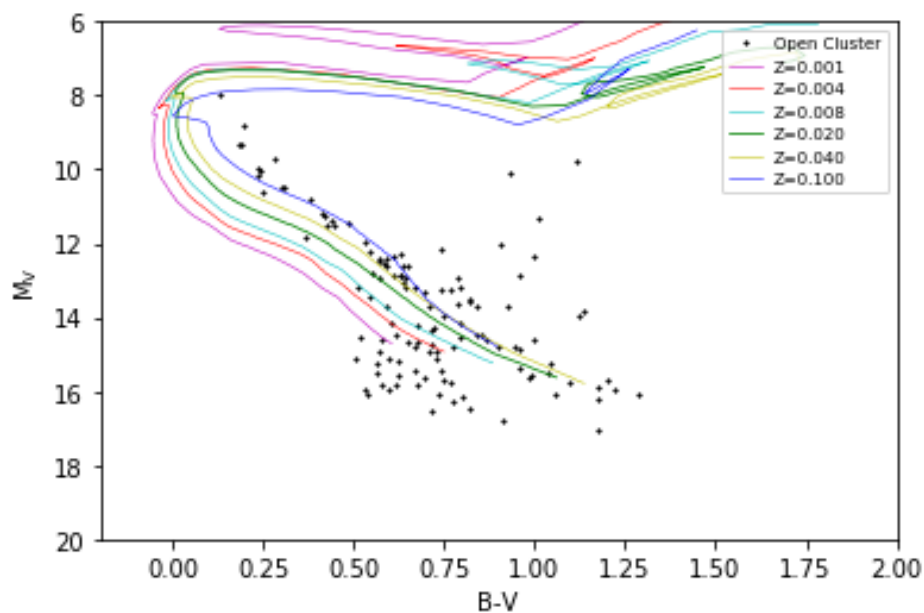


Figure 4.4: Determination of metallicity of open cluster

4.2 Globular Cluster

Three globular clusters GC1, GC2 and GC3 (fig. 4.5) were analyzed and their distance, age and metallicity was determined.

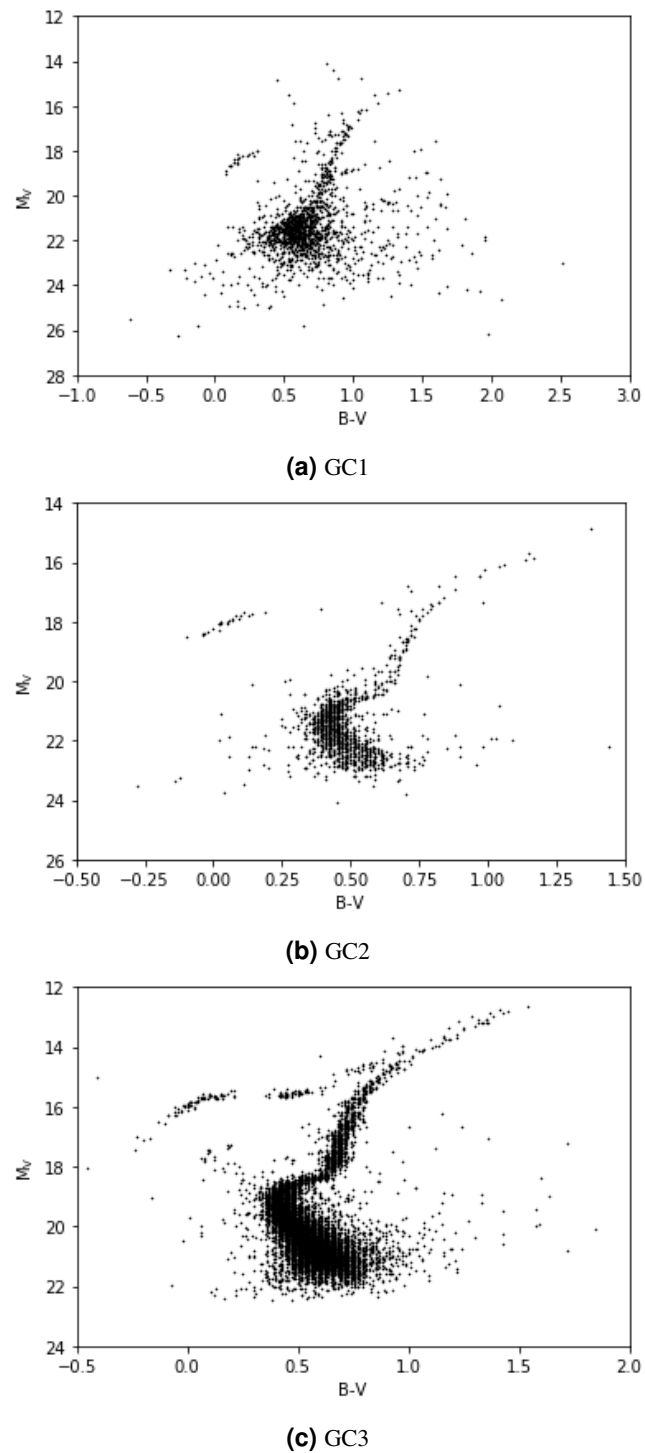


Figure 4.5: Globular clusters

4.2.1 Distance Determination

Globular clusters do not have an extended main sequence. Instead, the distance to old star clusters can be determined from the horizontal branch. The absolute magnitude of the horizontal branch is known to be $0.5 M_V$.

The position of the horizontal branch was determined as shown in fig. 4.6 and the distance was calculated using eq. (1.8). The extinction is again assumed to be zero.

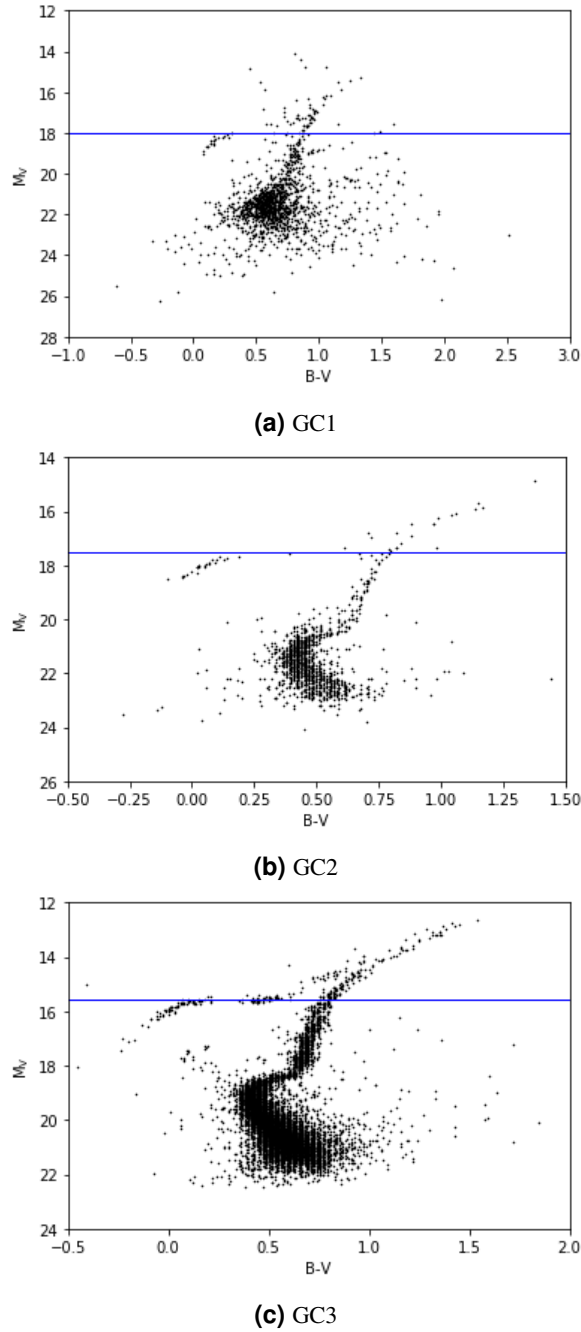


Figure 4.6: Horizontal branch of the globular clusters

The error in the distance modulus was found by looking at the stars on the horizontal branch deviating from our fit. The distances are summarized in table 4.1.

Cluster	m	d / kpc
GC1	18.5 ± 0.5	31.6 ± 7.3
GC2	17.5 ± 0.35	25.12 ± 4.05
GC3	15.55 ± 0.4	10.23 ± 1.89

Table 4.1: Distances of the globular clusters

4.2.2 Isochrone Fitting

Similar to the open cluster, the age is determined by the turn-off point and the metallicity by the main sequence. We did not get a good fit, so the best fit results were considered.

Age

We know that the globular clusters are old and have ages close to the age of the universe. We also notice many blue-stragglers. Blue-stragglers are stars at the turn-off point which are bluer than they are expected to be. This is explained by considering the collisions between stars thereby transferring mass to the older star enabling it to burn brighter. This can only happen long after the formation of the system as a whole [3]. This indicates that the cluster is very old. The fit is shown in fig. 4.7a. The ages are tabulated in table 4.2.

Metallicity

Globular clusters were formed early in time when the metal content in the universe was very low. So we expect them to have low metallicities. The fit is shown in fig. 4.7b. The metallicity of all three clusters was found to be 0.001.

Cluster	Age (Gyr)	Metallicity, Z
GC1	11.22 ± 1.30	0.001
GC2	12.59 ± 1.29	0.001
GC3	10 ± 5.64	0.001

Table 4.2: Age and metallicity of the globular clusters

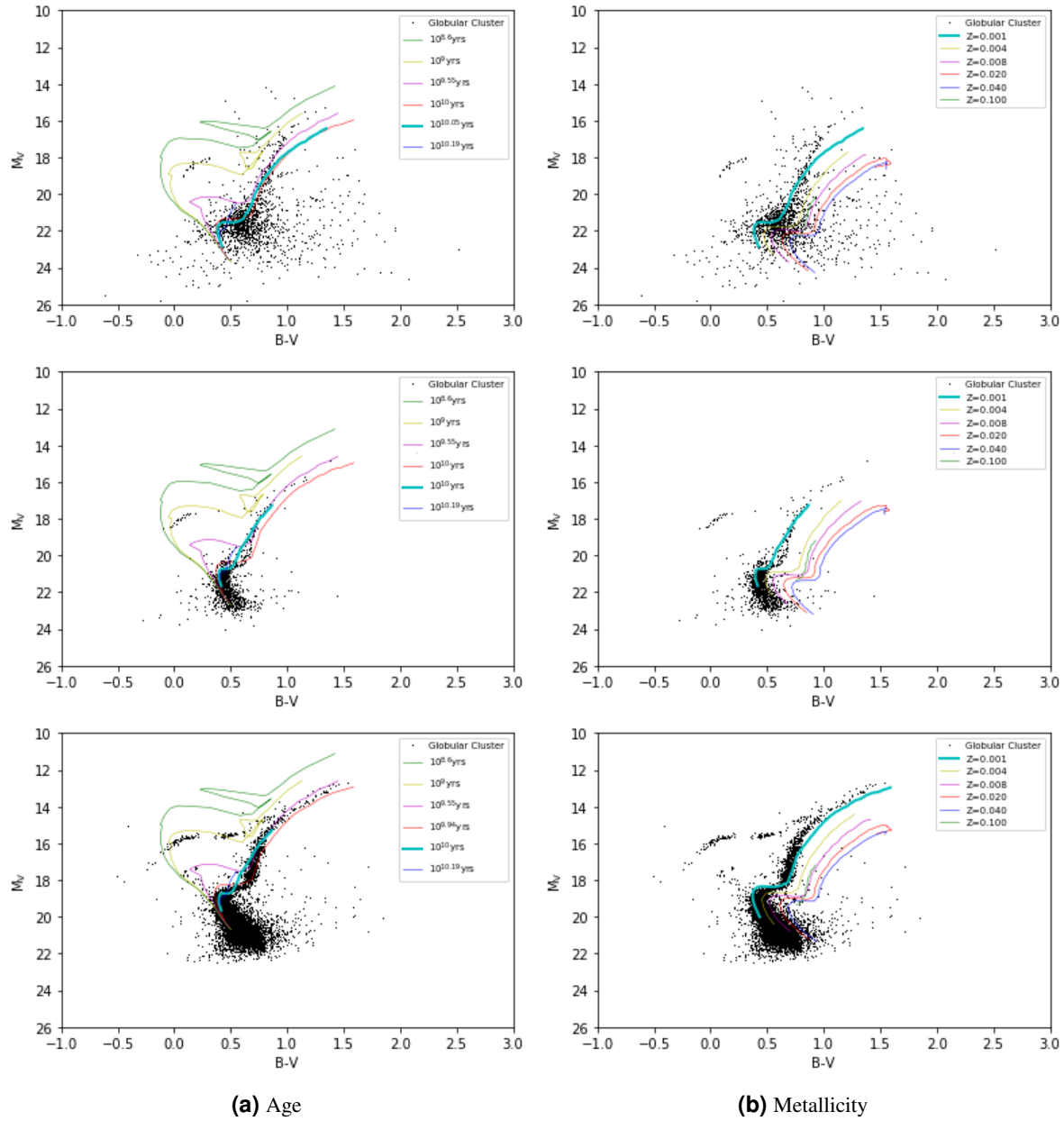


Figure 4.7: Determination of age and metallicity of globular clusters

5 Conclusion

One open cluster and three globular clusters were studied in this experiment. The results are summarized below.

Cluster	Distance (kpc)	Age (Gyr)	Metallicity, Z
Open cluster	416.87 ± 11.52	0.2457 ± 0.05155	0.1
GC1	31.6 ± 7.83	11.22 ± 1.30	0.001
GC2	25.12 ± 4.05	12.59 ± 1.29	0.001
GC3	10.23 ± 1.89	10 ± 5.64	0.001

Table 5.1: Age and metallicity of the globular clusters

As expected, the open cluster is young and has high metallicity. The globular clusters have low metallicity and are very old at the order of the age of the universe (13 Gyr).

Bibliography

- [1] Alberto Doria, Andreas Kupper, Xun Shi, Alex Tudorica & Jan Luca van den Busch: *Photometry of Star Clusters*: Script, 2017
- [2] <http://simbad.u-strasbg.fr/simbad/>
- [3] <http://astronomy.swin.edu.au/cosmos/B/Blue+Stragglers>

Exercises

T2.1

The probability of finding a star of mass less than $0.5M_{\odot}$ is:

$$\begin{aligned}\int_{0.08M_{\odot}}^{0.5M_{\odot}} \xi(m) dm &= \int_{0.08M_{\odot}}^{0.5M_{\odot}} 0.237 m^{-1.35} dm \\ &= 0.776015/M_{\odot}\end{aligned}$$

The number of stars with mass below $0.5M_{\odot}$ in a population of 1000000 stars is then:

$$0.776 \times 1000000 = 776015 \text{ stars}$$

The percentage of mass in stars below $0.5M_{\odot}$ is:

$$\int_{0.08M_{\odot}}^{0.5M_{\odot}} 0.237 m^{-1.35} \times mdm = 0.161755902$$

∴, the total mass in stars below $0.5M_{\odot}$ is:

$$0.161755902 \times 776015 = 1.26 \times 10^5 M_{\odot}$$

T2.2

1000 point sources $\implies N_s + N_{bin} = 1000$ and f_{bin} is known to be 0.7,

$$\therefore N_{bin} = f_{bin} \times (N_s + N_{bin}) = 700$$

$$\implies N_s = 1000 - 700 = 300$$

Then the total number of stars are:

$$N_s + 2N_{bin} = 300 + 1400 = 1700 \text{ stars}$$

T2.3

The angular size θ of an object with diameter d and at a distance D is given by:

$$\theta = \frac{d}{D}$$

- Globular cluster with $d = 50$ pc and at $D = 10 \times 10^3$ kc:

$$\theta = \frac{50}{10 \times 10^3} = (5 \times 10^{-3})^{\circ} = 18''$$

- Open cluster with $d = 5$ pc and at $D = 1 \times 10^3$ pc:

$$\theta = \frac{5}{1 \times 10^3} = (5 \times 10^{-3})^\circ = 18''$$

- Full moon with $d = 10^{-10}$ pc and at $D = 10^{-11} \times 10^3$ pc:

$$\theta = \frac{10^{-10}}{10^{-11} \times 10^3} = 0.01^\circ = 36''$$

T2.4

Flux, $f = N/t$ where N is the number of counts and t is the time of exposure. Here, we assume t is the same for both observations. Then, $f_R = 16000$, $m_R = 15.0$ and $f = 4000$. Using eq. (1.4),

$$m - m_R = -2.5 \log_{10}\left(\frac{f}{f_R}\right)$$

$$\begin{aligned} \implies m &= -2.5 \log_{10}\left(\frac{4000}{16000}\right) + 15.0 \\ &= 16.505 \end{aligned}$$

T2.5

$m = 16.505$ and $M = 10$. Using eq. (1.8) with $A = 0$,

$$\begin{aligned} d &= 10^{0.2(16.505-10+5)} \\ &= 199.99 \text{pc} \approx 200 \text{pc} \end{aligned}$$

T2.6

Using eq. (1.8) with $A = 0.2$,

$$\begin{aligned} d &= 10^{0.2(16.505-10+5-0.2)} \\ &= 182.39 \text{pc} \end{aligned}$$

T2.7

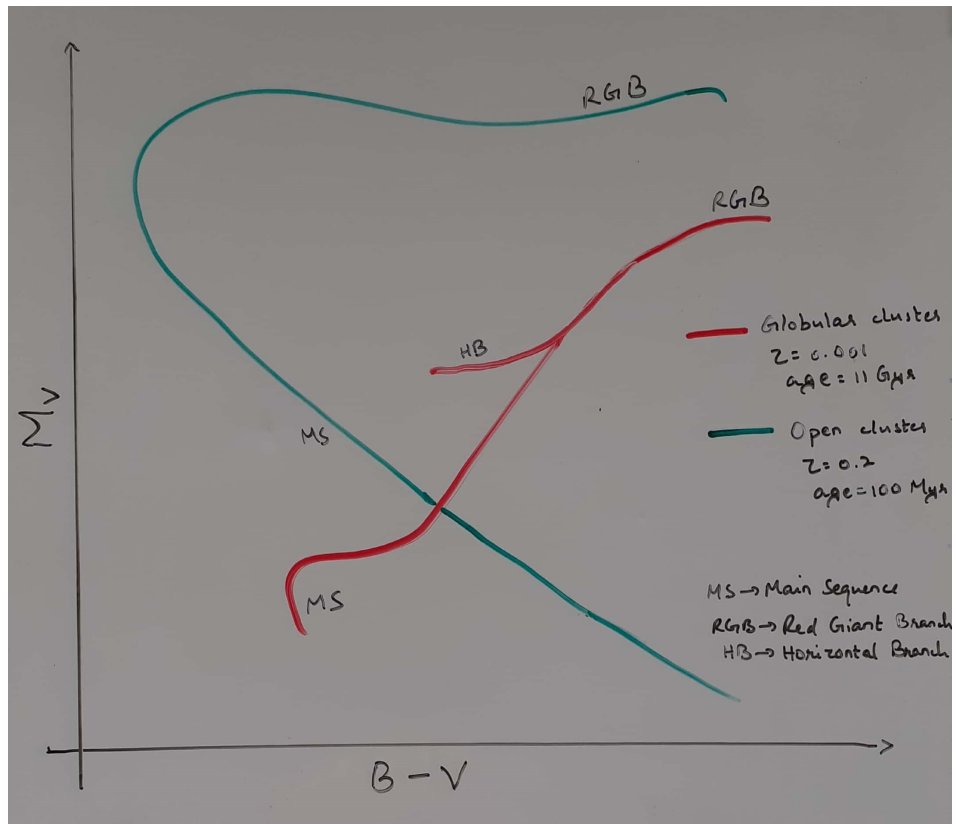


Figure 5.1: Schematic CMDs of one open and one globular cluster

T3.1

The f-number is the ratio of focal length f to the diameter of the pupil d ($= 50\text{cm}$). The Cassegrain focus has f-number $f/9$

$$\implies 9 = \frac{f_c}{50}$$

$$\therefore f_c = 450 \text{ cm} = 4.5 \text{ m}$$

and the primary focus has f-number $f/3$

$$\implies 3 = \frac{f_p}{50}$$

$$\therefore f_p = 150 \text{ cm} = 1.5 \text{ m}$$

T3.2

Consider a right-angled triangle with the radius of the CCD and the focal length as the two legs of the triangle. The angle subtended at the Cassegrain lens is:

$$\tan(\theta/2) = \frac{d/2}{f_c}$$

For $d = 3072 \times 9 \mu m$, we get:

$$\begin{aligned}\theta &= 2 \tan^{-1} \left(\frac{3072 \times 9 \times 10^{-6}}{2 \times 4.5} \right) \\ &= 6.144 \times 10^{-3} \text{ rad} \\ &= 0.352^\circ = 21'7''\end{aligned}$$

For $d = 2048 \times 9 \mu m$, we get:

$$\begin{aligned}\theta &= 2 \tan^{-1} \left(\frac{2048 \times 9 \times 10^{-6}}{2 \times 4.5} \right) \\ &= 4.096 \times 10^{-3} \text{ rad} \\ &= 0.235^\circ = 14'5''\end{aligned}$$

The total field of view is the total solid angle, $21'7'' \times 14'5'' = 297.39 \text{ sr}$.

The angular resolution is given by the size of the pixels. The minimum angular resolution is $\theta_{min} = 2 \tan^{-1} \left(\frac{1 \times 9 \times 10^{-6}}{2 \times 4.5} \right) = 0.41''$.

The angular resolution is limited by the diffraction effect on the incoming light which causes airy discs. This effect increases with decrease in pixel size.

T3.3

The factor 206 is obtained due to the conversion from radians to arcseconds as shown below:

$$\begin{aligned}\frac{\text{pixel size}/\mu m}{\text{focal length}/nm} &= \frac{\text{pixel size}/m}{\text{focal length}/m} \times 10^3 = 1 \text{ rad/pixel} \\ &= \left(1 \times \frac{180}{\pi} \right)^\circ/\text{pixel} \\ &= \left(\frac{180}{\pi} \times 60 \times 60 \right)''/\text{pixel} \\ &= (206.2 \times 10^3)''/\text{pixel} \\ \therefore \frac{\text{pixel size}/\mu m}{\text{focal length}/nm} &\approx 206''/\text{pixel}\end{aligned}$$

T3.4

$N_1 = 30000$ counts are obtained in 10s, then the flux of star 1 is $f_1 = 30000/10 = 3000$. Flux of star 2 is $f_2 = 30000/t_2$. Substituting in eq. (1.4):

$$\begin{aligned}3.0 - 5.0 &= -2.5 \log_{10} \left(\frac{3000}{30000/t_2} \right) \\ \implies \log_{10} \left(\frac{t_2}{10} \right) &= 0.8 \\ \therefore t_2 &= 63.1 \text{ s}\end{aligned}$$

T3.5

The size of the donuts indicate the distance of the dust particle from the camera. The smaller the

donut, the closer is the particle. It also tells us about the size of the dust particle.

T3.6

The full-well capacity of the CCD is $100000 e^-$ and its ADU gain is $1.4e^-/\text{ADU}$. Therefore, saturation is reached at:

$$\frac{100000}{1.4} = 71428.57 \text{ counts}$$

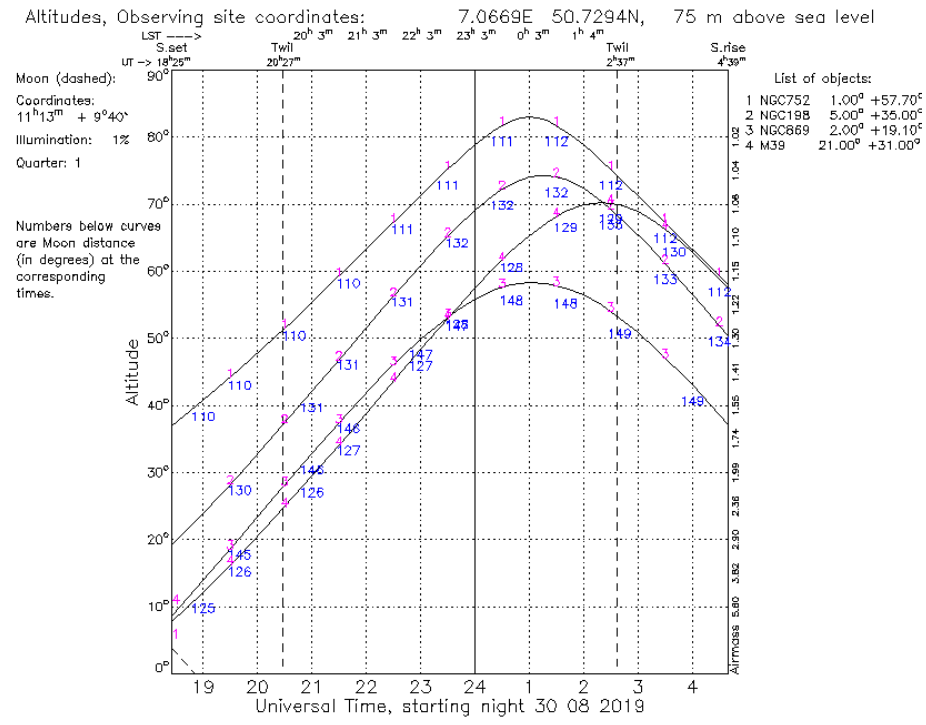
FLAT frames have 35714 counts at $1/2$ saturation and 47619 counts at $2/3$ saturation.

T4.1

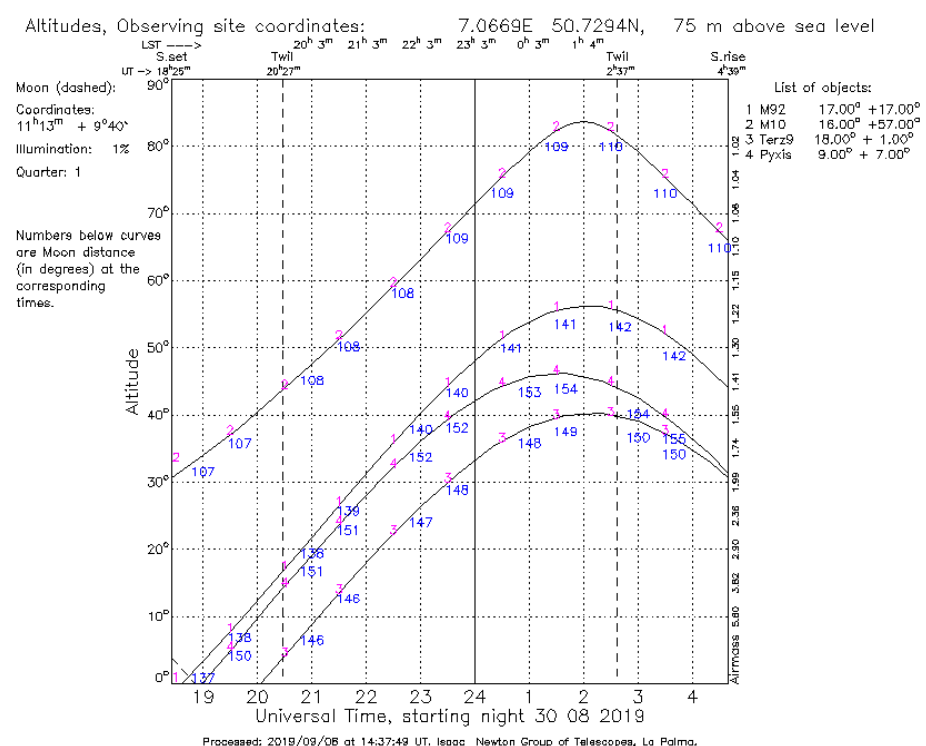
We did the observation on 30 August 2019 at around 21:30. The visibility plots for open and globular clusters are given in fig. 5.2a and fig. 5.2b respectively.

T4.2

We pick open cluster NGC 752 and globular cluster M10 as they have the highest altitudes.



(a) Visibility plot of open clusters



(b) Visibility plot of globular clusters